Hyperfinecourse A: electric quadrupole interaction

February 6, 2020

Abstract

This document is meant for optional background reading when studying www.hyperfinecourse.org. It deals with one of the chapters of this course. The formal course content is defined by the website and videos. The present document does not belong to the formal course content. It covers the same topics, but usually with more mathematical background, more physical background and more examples. Feel free to use it, as long as it helps you mastering the course content in the videos. If you prefer studying from the videos only, this is perfectly fine.

The present text has been prepared by Jeffrey De Rycke (student in this course in the year 2018-2019). He started from a partial syllabus written by Stefaan Cottenier for an earlier version of this course, and cleaned, edited and elaborated upon that material. That syllabus was itself inspired by a course taught by Michel Rots at KU Leuven (roughly 1990-1995).

1 From toy model to quantum physics

The writer of this document didn't think there was more background to add in addition to the course video about this topic. Writing about what is discussed in the video would be a literal translation from video to text, and this is not the purpose of these documents. For additional background on this video, please read https://biblio.ugent.be/publication/2988716/file/2988720.pdf. This is the paper from where said toy model originates and is writen by K. Rose and S. Cottenier (the lecturer of this course). The paper is free to download for everybody with a UGent account.

2 Quadrupole operator

As developed in Hyperfinecourse A: quantum version (equation 31), the leading correction term in the hamiltonian for the charge-charge interaction is:

$$\hat{H}_1 \;=\; \hat{H}_{qq} \;=\; -\frac{e^2 N Z}{5\epsilon_0}\left(\frac{1}{r_e^3}Y^2(\theta_e,\,\phi_e)\right)\cdot\left(r_n^2\,Y^2(\theta_n,\,\phi_n)\right) \tag{1}$$

In first order perturbation theory, we have to evaluate this in the eigenstates $\left|I\otimes\psi_e^{(0)}\right\rangle$ of the monopole hamiltonian $\hat{H}_0 \,=\, \hat{T}_n + \hat{U}_{nn} + \hat{H}_0$:

$$E_{qq} \;=\; -\left\langle\psi_e^{(0)}\otimes I\right|\frac{e^2 N Z}{5\epsilon_0}\left(\frac{1}{r_e^3}Y^2(\theta_e,\,\phi_e)\right)\cdot\left(r_n^2\,Y^2(\theta_n,\,\phi_n)\right)\left|I\otimes\psi_e^{(0)}\right\rangle \tag{2}$$

We do not consider charge-charge overlap, therefore we can separate the expression into:

$$E_{qq}^{(2)} \;=\; \langle I|\,{}_s\hat{Q}_{sh}^{(2)}\,|I\rangle\,\cdot\,\left\langle\psi_e^{(0)}\right|{}_s\hat{V}_{sh}^{(2)}\left|\psi_e^{(0)}\right\rangle \tag{3}$$

where we defined the nuclear electric quadrupole moment tensor operator (dimension Cm^2 or electron barn (eb))

$$\hat{Q}_q^2(\vec{r}_n) \,=\, eZ\sqrt{\frac{4\pi}{5}}\,r_n^2\,Y_q^2(\theta_n,\,\phi_n) \tag{4}$$

which operates on the nuclear space, and the electric quadrupole field tensor operator (or electric-field gradient tensor operator, dimension $\mathrm{V/m}^2$)

$$\hat{V}_q^2(\vec{r}_e) \,=\, -\frac{eN}{\sqrt{20\pi}\,\epsilon_0}\,\frac{1}{r_e^3}\,Y_q^2(\theta_e,\,\phi_e) \tag{5}$$

which operates on the electron space.

Let us not forget that expression 3 is a matrix. More precisely the matrix for the degenerate case of first order perturbation. It gives us information of the behaviour of the nucleus in the presence of the electric field gradient from the electrons.

2.1 The electric-field gradient operator

The matrix on the right in equation 3 is a tensor of rank two. It is symmetric and traceless and can therefore be described by 5 numbers. These 5 values can be calculated via ab initio code (which we do not discuss here), we will consider these 5 values as known. The 5 values depend on the choice of our axis system. Explicit expressions for the components of the cartesian forms of $Q_{sh}^{(2)}$ and $V_{sh}^{(2)}$ can be found by making the substitutions Hyperfinecourse A: quantum version (equation 17-21) in:

$$E_{pot}^{(2)} = \frac{1}{6}\int_1\int_2 \begin{bmatrix} 3x_1^2-r_1^2 & 3x_1y_1 & 3x_1z_1 \\ 3x_1y_1 & 3y_1^2-r_1^2 & 3y_1z_1 \\ 3x_1z_1 & 3y_1z_1 & 3z_1^2-r_1^2 \end{bmatrix} \cdot \frac{1}{r_2^5} \begin{bmatrix} 3x_2^2-r_2^2 & 3x_2y_2 & 3x_2z_2 \\ 3x_2y_2 & 3y_2^2-r_2^2 & 3y_2z_2 \\ 3x_2z_2 & 3y_2z_2 & 3z_2^2-r_2^2 \end{bmatrix} d\vec{r}_1 d\vec{r}_2 \tag{6}$$

or in (first dot product):

$$\begin{aligned} E_{pot}^{(2)} = {} & \frac{1}{6}\begin{bmatrix} \{3x_1^2\}-\{r_1^2\} & \{3x_1y_1\} & \{3x_1z_1\} \\ \{3y_1x_1\} & \{3y_1^2\}-\{r_1^2\} & \{3y_1z_1\} \\ \{3z_1x_1\} & \{3z_1y_1\} & \{3z_1^2\}-\{r_1^2\} \end{bmatrix} \cdot \\ & \begin{bmatrix} \frac{\partial^2 V_2(\vec{0})}{\partial x_1^2}-\frac{\Delta V_2(\vec{0})}{3} & \frac{\partial^2 V_2(\vec{0})}{\partial y_1 \partial x_1} & \frac{\partial^2 V_2(\vec{0})}{\partial z_1 \partial x_1} \\ \frac{\partial^2 V_2(\vec{0})}{\partial x_1 \partial y_1} & \frac{\partial^2 V_2(\vec{0})}{\partial y_1^2}-\frac{\Delta V_2(\vec{0})}{3} & \frac{\partial^2 V_2(\vec{0})}{\partial z_1 \partial y_1} \\ \frac{\partial^2 V_2(\vec{0})}{\partial x_1 \partial z_1} & \frac{\partial^2 f(\vec{0})}{\partial y_1 \partial z_1} & \frac{\partial^2 V_2(\vec{0})}{\partial z_1^2}-\frac{\Delta V_2(\vec{0})}{3} \end{bmatrix} + \\ & \frac{1}{6}\begin{bmatrix} \{r_1^2\} & 0 & 0 \\ 0 & \{r_1^2\} & 0 \\ 0 & 0 & \{r_1^2\} \end{bmatrix} \cdot \begin{bmatrix} \frac{\Delta V_2(\vec{0})}{3} & 0 & 0 \\ 0 & \frac{\Delta V_2(\vec{0})}{3} & 0 \\ 0 & 0 & \frac{\Delta V_2(\vec{0})}{3} \end{bmatrix} \end{aligned} \tag{7}$$

Using either expressions produces identical results only if there is no electron penetration in the nucleus. That was to be expected, as equation 4 was derived for the situation without penetration. The more general result obtained by equation 5 is:

$$\hat{V}_{ij} = -\frac{eN}{4\pi\epsilon_0}\frac{3x_{ie}x_{je}-r_e^3\delta_{ij}}{r_e^5} - \frac{\rho_e(\vec{0})}{3\epsilon_0}\delta_{ij} \tag{8}$$

The result for the quadrupole moment tensor does not depend on penetration being present or not:

$$\hat{Q}_{ij} = eZ\left(3x_{in}x_{jn}-r_n^3\delta_{ij}\right) \tag{9}$$

If we note $\left\langle \Psi_e^{(0)} \middle| \hat{V}_{ij} \middle| \Psi_e^{(0)} \right\rangle \equiv V_{ij}$, we can express the matrix elements of $\hat{V}^2$ as follows:

$$\left\langle \psi_e^{(0)} \middle| \hat{V}_0^2 \middle| \psi_e^{(0)} \right\rangle = \frac{1}{2}V_{zz}$$

$$\begin{aligned}
\left\langle \psi_e^{(0)} \right| \hat{V}_{\pm 1}^2 \left| \psi_e^{(0)} \right\rangle &= \mp \frac{1}{\sqrt{6}} \left(V_{xz} \pm V_{yz} \right) \\
\left\langle \psi_e^{(0)} \right| \hat{V}_{\pm 2}^2 \left| \psi_e^{(0)} \right\rangle &= \frac{1}{2\sqrt{6}} \left(V_{xx} - V_{yy} \pm i V_{xy} \right)
\end{aligned} \tag{10}$$

These matrix elements can be considerably simplified if we work in a principal axis system (PAS) for the electric-field gradient. For a crystalline solid this is something meaningful, as the lattice breaks the isotropy of space and provides special directions relative to which the PAS can be defined. The PAS is chosen such that the electric-field gradient tensor[1] at the point of the crystal we are interested in (the nucleus of the considered atom) is as simple as possible.

2.2 Intermezzo: Principal axis system rank 2 tensor

A principal axis system for a spherical tensor of rank 2 is an axis system in which the 3×3-matrix of the cartesian form of this tensor is diagonal (for symmetric matrices this is always possible). Once XYZ is rotated such that the matrix is diagonal, the axes are renamed by convention such that $|a_{zz}| \geq |a_{yy}| \geq |a_{xx}|$. The cartesian form in the PAS is now:

$$\begin{bmatrix} a_{xx} & 0 & 0 \\ 0 & a_{yy} & 0 \\ 0 & 0 & a_{zz} \end{bmatrix} \tag{11}$$

The trace of matrix is invariant upon rotation of the axis system and therefore remains zero. It means we have only 2 degrees of freedom in 11. Because there are also 3 degrees of freedom needed to specify the PAS with respect to the original XYZ (e.g. 3 Euler angles), we retain the 5 degrees of freedom expected for a spherical tensor of rank 2. Using the foreseen relations between cartesian and spherical components (Hyperfinecourse A: framework. Inverse relations of equations 27 and 28), we see that the spherical components in the PAS are:

$$\begin{aligned}
a_0^2 &= \frac{1}{2} a_{zz} \\
a_{\pm 1}^2 &= 0 \\
a_{\pm 2}^2 &= \frac{1}{2\sqrt{6}} \left(a_{xx} - a_{yy} \right)
\end{aligned} \tag{12}$$

Because $a_{+2}^2 = a_{-2}^2$ also in the spherical components only 2 apparent degrees of freedom are left. Again because of the 3 degrees of freedom needed to specify the PAS, we find back the 5 degrees of freedom which are needed.

$$\left\langle \psi_e^{(0)} \right| \hat{V}_0^2 \left| \psi_e^{(0)} \right\rangle = \frac{1}{2} V_{zz}$$

[1] Attention: not the *tensor operator*, which is something we cannot change (it is as it is), but the electric-field gradient *tensor* itself, i.e. the expectation value of the electric-field gradient tensor operator.

$$\begin{aligned} \left\langle \psi_e^{(0)} \right| \hat{V}_{\pm 1}^2 \left| \psi_e^{(0)} \right\rangle &= 0 \\ \left\langle \psi_e^{(0)} \right| \hat{V}_{\pm 2}^2 \left| \psi_e^{(0)} \right\rangle &= \frac{1}{2\sqrt{6}} \left(V_{xx} - V_{yy} \right) \end{aligned} \tag{13}$$

The 3 axes of the PAS are named such that $|V_{zz}| \geq |V_{yy}| \geq |V_{xx}|$. Be aware that the PAS is dependent on $\left|\psi_e^{(0)}\right\rangle$: it is not something universal, but depends on the particular compound you examine! Because of the condition on the trace of the cartesian form (traceless), only two degrees of freedom are left in 13. We can write this explicitly by defining a parameter η:

$$\eta = \frac{V_{xx} - V_{yy}}{V_{zz}} \tag{14}$$

which fulfills the relation $0 \leq \eta \leq 1$. With this definition we can write the spherical components in the PAS as:

$$\begin{aligned} \left\langle \psi_e^{(0)} \right| \hat{V}_0^2 \left| \psi_e^{(0)} \right\rangle &= \frac{1}{2} V_{zz} \\ \left\langle \psi_e^{(0)} \right| \hat{V}_{\pm 1}^2 \left| \psi_e^{(0)} \right\rangle &= 0 \\ \left\langle \psi_e^{(0)} \right| \hat{V}_{\pm 2}^2 \left| \psi_e^{(0)} \right\rangle &= \frac{1}{2\sqrt{6}} \eta V_{zz} \end{aligned} \tag{15}$$

Only η and V_{zz} determine the electric-field gradient, indeed 2 degrees of freedom. The 3 other degrees of freedom expected for a spherical tensor of rank 2 are used to specify the PAS with respect to the original axis system, e.g. by 3 Euler angles. One calls η the *asymmetry parameter* of the electric-field gradient. The reason is that for $\eta = 0$ the xx- and yy-components of the cartesian form are equal: the gradient of the electric field is the same in all directions in the XY-plane, hence the electric-field gradient has axial symmetry about the Z-axis[2]. The more η deviates from 0 and approaches 1, the more the gradient of the electric field becomes stronger in the y-direction compared to the x-direction (the gradient in the z-direction remains the strongest of course).

[2]This can be seen also in the spherical component: only V_0^2 is not zero, hence there is axial symmetry.

2.3 The nuclear electric quadrupole moment operator

Let us now look to the first term in equation 3. Again we are faced with the problem that we do not know explicit expressions for the nuclear many-body wave functions $|I\rangle$. As for the 3 components of the magnetic dipole operator, we will transform the 5 components of the electric quadrupole moment operator $\hat{Q}^2_q(\vec{r}_n)$ into expressions that involve an experimentally observable scalar – 'the' quadrupole moment Q – and operators for which we can calculate the matrix elements in the $|I\rangle$ basis. They will depend on the (experimentally known) value of I. In contrast to the magnetic case, the $|I, m\rangle$ will not be eigen states of the hamiltonian, such that non-diagonal matrix elements will be present. The transformation takes somewhat more effort than for the magnetic case, and starts from the Wigner-Eckart theorem. This famous theorem states that the matrix elements of all spherical tensors of rank n are proportional, because they can be written as:

$$<I',\, m'_I|\, T^n_q|\, I,\, m_I> = (-1)^{I'-m'_I} \begin{pmatrix} I' & n & I \\ -m'_I & q & m_I \end{pmatrix} <I' \,||\, T^n \,||\, I> \qquad (16)$$

(The so-called reduced matrix element $< I' \,||\, T^n \,||\, I >$ is independent of m'_I, m_I and q, and the Wigner $3j$-symbol between large parentheses has a close relationship[3] to the Clebsch-Gordan coefficients.) Indeed, the same type of matrix element of a spherical tensor A^n of the same rank is:

$$<I',\, m'_I|\, A^n_q|\, I,\, m_I> = (-1)^{I'-m'_I} \begin{pmatrix} I' & n & I \\ -m'_I & q & m_I \end{pmatrix} <I' \,||\, A^n \,||\, I> \qquad (18)$$

and therefore

$$\frac{<I',\, m'_I|\, T^n_q|\, I,\, m_I>}{<I',\, m'_I|\, A^n_q|\, I,\, m_I>} = \frac{<I' \,||\, T^n \,||\, I>}{<I' \,||\, A^n \,||\, I>} = C \qquad (19)$$

with C a constant depending on I', I and n, but not on m_I, m'_I and q.

The tensor operators $r^2_n\, Y^2(\theta_n,\, \phi_n)$ and $I^2\, Y^2(\vec{I})$ can be shown to be both[4] spherical tensor operators of rank 2. Applying equation 19 we get:

$$<I',\, m'_I|\, r^2_n\, Y^2(\theta_n,\, \phi_n)\,|\, I,\, m_I> = C\ <I',\, m'_I|\, I^2\, Y^2(\vec{I})\,|\, I,\, m_I> \qquad (20)$$

With this equation, we can write the matrix elements of $\hat{Q}^2_q(\vec{r}_n)$ in terms of $I^2\, Y^2(\vec{I})$. But then we need explicit expressions for $Y^2_q(\vec{I})$. For $q = 0$ and with

[3] The exact relation is:

$$\begin{pmatrix} j_1 & j_2 & j_3 \\ m_1 & m_2 & m_3 \end{pmatrix} = (-1)^{j_1 - j_2 - m_3}\, \frac{1}{\sqrt{2j_3+1}}\, (j_1\, j_2\, m_1\, m_2\,|\, j_1\, j_2\, j_3\, m_3) \qquad (17)$$

One often uses $3j$-symbols instead of Clebsch-Gordan coefficients because the former have nicer symmetry properties.

[4] Interpret the notation $Y^2(\vec{I})$ as follows: in $Y^2(\theta_n,\, \phi_n)$ (or $Y^2(\vec{r})$), θ_n and ϕ_n give the direction of $\vec{r}_n$. Use therefore in $Y^2(\vec{I})$ as argument for Y^2 the angles which specify the direction of $\vec{I}$.

θ and ϕ giving the direction of a position vector $\vec{r}$, we can with $\cos\theta = z/r$ write Y_0^2 as[5]:

$$Y_0^2(\theta,\,\phi) \;=\; Y_0^2(\vec{r}) \,=\, \frac{1}{2}\sqrt{\frac{5}{4\pi}}\,\left(\frac{3z^2\,-\,r^2}{r^2}\right) \tag{23}$$

$$r^2\,Y_0^2(\vec{r}) \;=\; \frac{1}{2}\sqrt{\frac{5}{4\pi}}\,\left(3z^2\,-\,r^2\right) \tag{24}$$

x, y an z are the x-, y- and z-components of $\vec{r}$. If we note the x-, y- and z-components of $\vec{I}$ as I_x, I_y and I_z, we can by analogy write:

$$I^2\,Y_0^2(\vec{I}) \;=\; \frac{1}{2}\sqrt{\frac{5}{4\pi}}\,\left(3I_z^2\,-\,I^2\right) \tag{25}$$

Show yourself that:

$$I^2\,Y_{\pm1}^2 \;=\; \mp\sqrt{\frac{15}{8\pi}}\,\frac{1}{2}\,\left(I_zI_\pm + I_\pm I_z\right) \tag{26}$$

$$I^2\,Y_{\pm2}^2 \;=\; \frac{1}{4}\sqrt{\frac{15}{2\pi}}\,I_\pm^2 \tag{27}$$

The operators $\hat{I}_+$ and $\hat{I}_-$ are defined in hyperfinecourse A: magnetic hyperfine interaction (equations 16 and 17).

Our last task before having found the nuclear matrix elements, is to search for the value of the proportionality constant C. First we define similarly the *observable* quadrupole moment Q of the nucleus:

$$Q \;=\; Z\,<I,\,m_I = I|\,3z^2 - r^2|\,I,\,m_I = I> \tag{28}$$

$$\;=\; Z\,2\sqrt{\frac{4\pi}{5}}\,<I,\,I|\,r_n^2 Y_0^2(\vec{r})|\,I,\,I> \tag{29}$$

Note the difference between this definition (just a number) and the quadrupole tensor (5 components). Following general practice, we define this observable quadrupole moment in units of m^2, and not in units of Cm^2 as we did for the quadrupole moment tensor (equation 4). Numerical values for Q are usually given in *barn* (1 barn = 1 b = 10^{-28} m^2, typical values are 0 - 100 b). The corresponding unit for the tensor $Q_q^{(2)}$ is the *electron barn* (eb)[6].

[5]

$$Y_0^2\,(\theta,\,\phi) \;=\; \sqrt{\frac{5}{4\pi}}\,\left(\frac{3}{2}\cos^2\theta - \frac{1}{2}\right) \tag{21}$$

(22)

[6]Do not confuse the electron barn with the *Coulomb barn* (Cb), which is not used in practice. 1 eb = $1.602\cdot10^{-19}$ Cb = $1.602\cdot10^{-47}$ Cm^2.

Apply now Wigner-Eckart to the definition of Q:

$$Q = Z\,2\sqrt{\frac{4\pi}{5}} \begin{pmatrix} I & 2 & I \\ -I & 0 & I \end{pmatrix} <I \,||\, r_n^2 Y^2(\vec{r})||\, I> \tag{30}$$

and hence:

$$<I \,||\, r_n^2 Y^2(\vec{r})||\, I> = \frac{Q}{Z\,2\sqrt{\frac{4\pi}{5}} \begin{pmatrix} I & 2 & I \\ -I & 0 & I \end{pmatrix}} \tag{31}$$

which expresses the reduced matrix element of $r_n^2\, Y^2(\vec{r_n})$ as a function of observable quantities. Now apply Wigner-Eckart again, on the following matrix element of the other operator:

$$<I,\, I|\, I^2 Y_0^2(\vec{I})|\, I, I> = \begin{pmatrix} I & 2 & I \\ -I & 0 & I \end{pmatrix} <I \,||\, I^2 Y^2(\vec{I})||\, I> \tag{32}$$

On the other hand, also this is true:

$$<I,\, I|\, I^2 Y_0^2(\vec{I})|\, I, I> = \frac{1}{2}\sqrt{\frac{5}{4\pi}}\; <I,\, I|\, 3I_z^2 - I^2|\, I, I> \tag{33}$$

$$= \frac{1}{2}\sqrt{\frac{5}{4\pi}}\,\hbar^2\left(3I^2 - I(I+1)\right) \tag{34}$$

$$= \frac{1}{2}\sqrt{\frac{5}{4\pi}}\,\hbar^2\;\left(I\,(2I-1)\right) \tag{35}$$

Combining 32 with 35 gives the reduced matrix element of $I^2\, Y^2(\vec{I})$, which together with 31, 19 and 20 finally yields the desired constant:

$$C = \frac{Q}{Z\,\hbar^2\,(I(2I-1))} \tag{36}$$

We can now finally express the quadrupole moment operator in terms of Q and the operators $\hat{I}^2$, $\hat{I}_z$ and $\hat{I}_\pm$:

$$\hat{Q}_q^2 = \sqrt{\frac{4\pi}{5}}\frac{eQ}{I\,(2I-1)\,\hbar^2}\,\hat{\vec{I}}^2\, Y_q^2(\hat{\vec{I}}) \tag{37}$$

with $\hat{\vec{I}}^2\, Y_q^2(\hat{\vec{I}})$ given by equations 25 to 27.

All this enables us to write down explicitly the nuclear matrix elements:

$$<I,\, m_I'|\, Q_0^2\,|\, I,\, m_I> = \tag{38}$$
$$\frac{1}{2}\,\frac{e\,Q}{I(2I-1)}\;\left(3m^2 - I(I+1)\right)\;\delta_{m_I,\, m_I'}$$

$$<I,\, m'_I|\, Q^2_{\pm 1}\,|\, I,\, m_I> = \tag{39}$$
$$\mp\,\frac{1}{2}\,\sqrt{\frac{3}{2}}\,\frac{e\,Q}{I(2I-1)}\,\sqrt{I(I+1)\,-\,m_I(m_I\pm 1)}\,(2m_I\,\pm 1)\,\delta_{m'_I,\,m_I+1}$$
$$<I,\, m'_I|\, Q^2_{\pm 2}\,|\, I,\, m_I> = \tag{40}$$
$$\frac{1}{2}\,\sqrt{\frac{3}{2}}\,\frac{e\,Q}{I(2I-1)}\,\sqrt{(I(I+1)-m_I(m_I\pm 1))\,(I(I+1)-(m_I\pm 1)(m_I\pm 2))}\,\delta_{m'_I,\,m_I+2}$$

The observable nuclear quadrupole moment Q as defined by equation 29 is an experimentally accessible measure for the deviation from spherical symmetry of the nucleus. We can make the observation that due to equations 20, 29 and 35, Q is zero for $I = 0$ and $I = 1/2$, which means that these nuclei are always spherically symmetric. As a result, all nuclear matrix elements are zero in these two cases, and the quadrupole hamiltonian will not yield any energy contribution. The lowest spin for which a quadrupole contribution to the total energy is observable is therefore $I = 1$. Similar arguments can be used to prove that the lowest spin for which a hexadecapole moment can exist is $I = 3/2$.

2.4 Energy levels of the electric quadrupole hamiltonian for solids

By inserting equations 37 and equations 15 into equation 3, we obtain the equivalent of equation 31 in hyperfinecourse A: magnetic hyperfine interaction: a Hamiltonian that describes the energy contribution due to the interaction between a specific electric-field gradient tensor (specified by V_{zz}, η and the orientation of its PAS with respect to the crystal) and the nuclear quadrupole moment tensor, depending on the orientation of the latter with respect to the PAS:

$$H^{nuc}_{qq} \;=\; \frac{e\,Q\,V_{zz}}{4\,I(2I-1)\,\hbar^2}\,\left[(3I_z^2-I^2)\,+\,\frac{\eta}{2}\,(I_+^2+I_-^2)\right] \tag{41}$$

This hamiltonian depends on the electric-field gradient through V_{zz} and η, and on the spin of the nucleus through I. It also depends on the orientation of the nucleus (m_I), through $\hat{I}_z$ and $\hat{I}^2_{\pm}$. As the unperturbed Hamiltonian $\hat{T}_n + \hat{U}_{nn} + \hat{H}_0$ does not depend on m_I, we should use first order perturbation theory for the degenerate case. In contrast to the magnetic case, the matrix formed by $\langle m'_I,\, I|\, H^{nuc}_{qq}\,|I,\, m_I\rangle$ is not diagonal, due to the presence of $\hat{I}_{\pm}$. Therefore, it must be diagonalized in order to find the eigenvalues and eigenfunctions. The only – and important – exception is when the electric-field gradient has axial symmetry ($\eta = 0$). We examine now the eigenstates and eigenvalues of H^{nuc}_{qq} with and without axial symmetry of the electric-field gradient.

3 Case studies & symmetry

3.1 Analytical example 1: I = 3/2

We will search now explicit and analytical expressions for eigen values and eigen functions of a non-axially symmetric quadrupole hamiltonian for the case $I = 3/2$. These eigen states $|N>$ are not the $|I, m_I>$, but because the latter form a basis the equality

$$\sum_{m_I} |I, m_I><I, m_I| \;=\; 1 \tag{42}$$

holds, and this we can use to decompose $|N>$ in the $|I, m_I>$-basis:

$$|N> = \sum_{m_I} \underbrace{<I, m_I|N>}_{c_{m_I}} |I, m_I> \tag{43}$$

Our goal is to find the coefficients c_{m_I} [7].

The non-zero matrix elements of H^{nuc}_{qq} in the $|I, m_I>$-basis are[8]:

$$<\pm\frac{1}{2}|\, H^{nuc}_{qq}|\, \pm\frac{1}{2}> \;=\; -3\,\frac{eQ\,V_{zz}}{12} \tag{44}$$

$$<\pm\frac{3}{2}|\, H^{nuc}_{qq}|\, \pm\frac{3}{2}> \;=\; +3\,\frac{eQ\,V_{zz}}{12} \tag{45}$$

$$<\pm\frac{3}{2}|\, H^{nuc}_{qq}|\, \mp\frac{1}{2}> \;=\; \sqrt{3}\,\eta\,\frac{eQ\,V_{zz}}{12} \tag{46}$$

The full matrix reads:

$$E_Q \;=\; \frac{eQ\,V_{zz}}{12} \begin{array}{c} [+\frac{3}{2} \quad +\frac{1}{2} \quad -\frac{1}{2} \quad -\frac{3}{2}] \\ \left[\begin{array}{cccc} 3 & 0 & \sqrt{3}\,\eta & 0 \\ 0 & -3 & 0 & \sqrt{3}\,\eta \\ \sqrt{3}\,\eta & 0 & -3 & 0 \\ 0 & \sqrt{3}\,\eta & 0 & 3 \end{array}\right] \end{array} \tag{47}$$

One can find now the eigen vectors and eigen values of this matrix in the usual way. The secular equation would be a fourth order polynomial. We can reduce the complexity however just by making a rearrangement of the basis states in the following way:

$$E_Q \;=\; \frac{eQ\,V_{zz}}{12} \begin{array}{c} [+\frac{3}{2} \quad -\frac{1}{2} \quad -\frac{3}{2} \quad +\frac{1}{2}] \\ \left[\begin{array}{cccc} 3 & \sqrt{3}\,\eta & 0 & 0 \\ \sqrt{3}\,\eta & -3 & 0 & 0 \\ 0 & 0 & 3 & \sqrt{3}\,\eta \\ 0 & 0 & \sqrt{3}\,\eta & -3 \end{array}\right] \end{array} \tag{48}$$

[7] Clearly, if $\eta = 0$ all c_{m_I} are zero except for one which equals 1.
[8] We note for a while $|I, m_I>$ as $|m_I>$.

In this notation we clearly see that the new eigen states will be combinations of either $|\frac{3}{2}, +\frac{3}{2}>$ and $|\frac{3}{2}, -\frac{1}{2}>$ only, or $|\frac{3}{2}, -\frac{3}{2}>$ and $|\frac{3}{2}, +\frac{1}{2}>$ only. The problem is reduced now to finding the eigenvalues and eigenstates of two identical smaller matrices (the secular equations will be twice a second order polynomial here). We will see soon that this kind of reduction is a general property. Verify that both submatrices have as eigen values:

$$E_a \;=\; E_{\pm\tilde{\frac{3}{2}}} \;\;=\;\; \frac{eQ\,V_{zz}}{4}\sqrt{1+\frac{\eta^2}{3}} \tag{49}$$

$$E_b \;=\; E_{\pm\tilde{\frac{1}{2}}} \;\;=\;\; -\,\frac{eQ\,V_{zz}}{4}\sqrt{1+\frac{\eta^2}{3}} \tag{50}$$

As both eigenvalues appear twice in the full 4×4-matrix, we say they have a multiplicity of 2.

3.2 Analytical example 1: I = 1

By a suitable rearrangement, we can write the full matrix – similarly to equation 48 – as follows:

$$E_Q \;=\; \frac{eQ\,V_{zz}}{4} \begin{array}{c} \begin{array}{ccc} [+1 & -1 & 0] \end{array} \\ \begin{bmatrix} 1 & \eta & 0 \\ \eta & 1 & 0 \\ 0 & 0 & -2 \end{bmatrix} \end{array} \tag{51}$$

We immediately recognizes an eigenvalue $E_{\tilde{0}}$ which is identical to the eigenvalue $E_{m_I=0}$ for the case of axial symmetry, and which does not depend on η. The eigen state belonging to $E_{\tilde{0}}$ is identical to $|\,0>$:

$$E_{\tilde{0}} \;=\; -\,\frac{eQ\,V_{zz}}{2} \qquad |\,\tilde{0}> = \,|\,0> \tag{52}$$

Non-axial symmetry will therefore not change this state.

The eigenvalues of the 2×2 submatrix do depend on η:

$$E_\pm \;\;=\;\; \frac{eQ\,V_{zz}}{4}\,(1 \pm \eta) \tag{53}$$

$$|\pm> \;\;=\;\; \frac{1}{\sqrt{2}}\,(|+1> \pm |-1>) \tag{54}$$

The difference

$$E_+ - E_- \;=\; \frac{eQ\,V_{zz}}{2}\,\eta \tag{55}$$

is linear in η.

3.3 Symmetry properties and classes

We observe the following two facts:

- The expectation values of $|\, I,\, \pm m_I >$ are identical under H_{qq}^{nuc}. Indeed, the following symmetry relations are valid:

$$<I,\, m_I + 2|\, I_+^2\,|\, I, m_I> \;=\; <I,\, -m_I - 2|\, I_-^2\,|\, I, -m_I> \qquad (56)$$

$$<I,\, m_I|\, 3I_z^2 - I^2|\, I,\, m_I> \;=\; <I,\, -m_I|\, 3I_z^2 - I^2|\, I,\, -m_I> \qquad (57)$$

  and therefore:

$$<I,\, m_I|\, H_{qq}^{nuc}|\, I,\, m_I> \;=\; <I,\, -m_I|\, H_{qq}^{nuc}|\, I,\, -m_I> \qquad (58)$$

- Because H_{qq}^{nuc} connects only states with $\Delta m_I = 0$ and $\Delta m_I = \pm 2$, the states can be divided in 2 classes, such that no state of one class can ever be connected to a state of the other class. The situation is different for integer and half integer spin:

  – integer spin:

$$\textit{Class 1}: \quad m_I \;=\; \textit{even} \qquad (59)$$

$$\textit{Class 2}: \quad m_I \;=\; \textit{odd} \qquad (60)$$

  – half integer spin

$$\textit{Class 1}: \quad m_I \;=\; -I,\; -I+2,\; \ldots,\; +\frac{1}{2},\; +\frac{5}{2},\; \ldots, I-1 \qquad (61)$$

$$\textit{Class 2}: \quad m_I \;=\; -I+1,\; -I+3,\; \ldots,\; -\frac{1}{2},\; +\frac{3}{2},\; \ldots, +I \qquad (62)$$

The existence of these two classes means that it is always possible to rearrange the eigenstates in such a way that H_{qq}^{nuc} is in block form, because the block form explicitly shows that only states belonging to the same class can be mixed. In our two examples above, we did indeed observe that this was possible. The situation is qualitatively different however for integer and half integer spin:

half integer spin: The number of states in both classes is the same, the two submatrices have therefore the same dimension. Even better, by virtue of the symmetry properties 56 and 57, both submatrices are identical[9] The states $|\, m_I >$ and $|\, -m_I >$ play exactly the same role, each for their one submatrix.

Consider now an eigenstate $|\, N_1 >$ of H_{qq}^{nuc}. It must be built from states $|\, m_I >$ belonging to one and the same class, and according to equation 43 the coefficients c_{m_I} with m_I belonging to the other class are zero. For half

[9] You can convince yourself about this by looking at 48, and by making the matrix for $I = 5/2$. It is not necessary to write down explicit matrix elements, just use 56 and 57 to identify identical ones.

integer spin, m_I and $-m_I$ belong to different classes. Therefore, if $c_{m_I}^{N_1}$ appears in the development of $|\, N_1>$, $c_{-m_I}^{N_1}$ must be zero. But because the two submatrices are identical and because $|\, \pm m_I>$ play the same role, there must exist an eigenstate $|\, N_2>$ of H_{qq}^{nuc} built from the corresponding states of the other class, with the same coefficients: $c_{-m_I}^{N_2} = c_{m_I}^{N_1}$ and $c_{m_I}^{N_2} = 0 = c_{-m_I}^{N_1}$.

Because $|\, N_1>$ and $|\, N_2>$ are eigenstates of identical submatrices, they must have identical eigenvalues (-energies) and are therefore degenerate. This reasoning does not depends on the value of η, and we can conclude: *the eigenstates of H_{qq}^{nuc} for half integer I are two-fold degenerate (Kramers-degeneracy).* The degeneracy which was present for axial symmetry is never lifted for half integer spin.

integer spin: In this case, there will always be a different number of states in each class. The two submatrices will have a different dimension and can hence never be the identical. The states $|\, \pm m_I>$ now belong to the same class. Therefore there is no reason why they must lead to degenerate states (although they still can do so). In general, the $\pm m_I$-degeneracy will be lifted for integer spin.

If I becomes larger, the dimension of the submatrices grows and hence also the degree of the secular equation. From $I = 4$ onwards, one deals with secular equations of the fifth degree and higher. It is well known from algebra that only for polynomials up to the fourth degree analytical formulae for their roots exist. For higher orders numerical procedures are the only possibility. This means that $I = 7/2$ is the highest spin for which the eigenvalues can be given analytically (although already from $I = 5/2$ onwards the analytical solution becomes quite involved). In fig. 1 the eigenvalues of H_{qq}^{nuc} (found either analytically or numerically) for some values of I are given as a function of η. Note the Kramers degeneracy for half integer spin, and the fast lifting of degeneracy for $m_I = \pm 1$ (remember it was present already in first order perturbation theory!). The larger $|\, m_I|$, the higher η needs to be in order to produce a sufficiently large splitting.

One can compare these pictures of fig. 1 to fig. 2 of the gravitational example. There all possible orientations of the dumb-bell (= nucleus) were allowed. In the quantummechanical case only a limited number of orientations remains, which means that we must select a discrete number of energies from the continuous range of fig. 2.

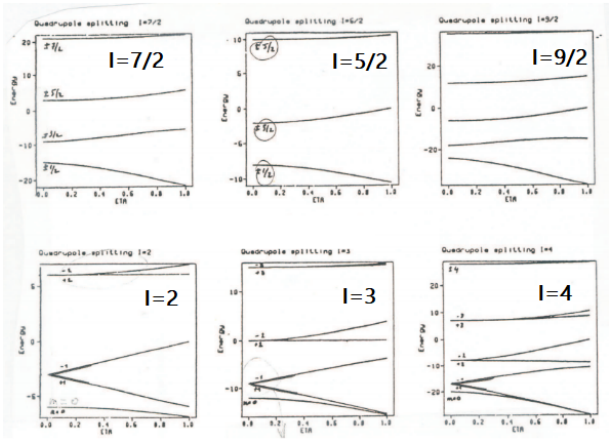

Figure 1: *Quadrupole splittings for half integer (top, 7/2, 5/2, 9/2) and integer (bottom, 2, 3, 4) spins. The vertical energy axis is in units of* $eQV_{zz}/I(2I-1)$*, while the horizontal axis scans all possible values of the asymmetry parameter* η $(0 \rightarrow 1)$*.*

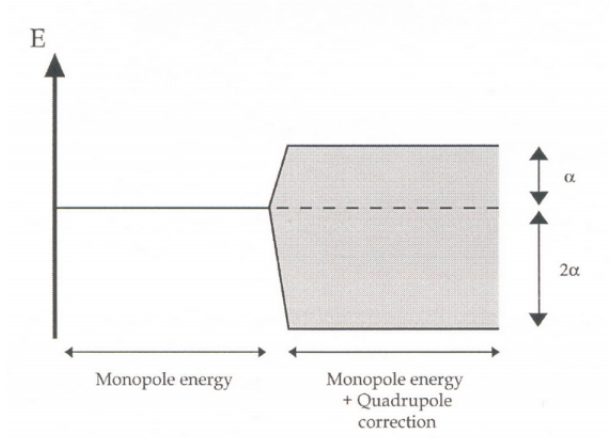

Figure 2: *See hyperfinecourse A: framework, Figure 9*

3.4 Symmetry properties of the electric-field gradient

For the magnetic hyperfine field we were able to identify where in a crystal such a field can exist and what will be its direction, just by using symmetry arguments. In the present section we will show how the crystallographic symmetry can be used to identify sites where an electric-field gradient exists, and what is the direction of the Z-axis of its PAS.

3.5 Theorem 1: an n-fold rotation axis

Consider a spherical tensor of rank 2 V^2 in an axis system $S1$. Its 5 components $V^2_{q'}(S1)$ are related to the component $V^2_q(S2)$ in an axis system $S2$ in the following way:

$$V^2_q(S2) \;=\; \sum_{q'} D^{(2)}_{q'q}\,(\alpha,\,\beta,\,\gamma)\,V^2_{q'}(S1) \tag{63}$$

The quantities $D^{(2)}_{q'q}\,(\alpha,\,\beta,\,\gamma)$ are components of the *Wigner rotation matrix* of dimension $2\cdot 2+1$ which can be found in tables. The angles α, β and γ are the Euler angles which specify $S2$ with respect to $S1$.

Consider now a position in a crystal of whom the point group contains an n-fold rotation axis. Imagine we know the 5 electric field gradient components in an axis system $S1$ with its z-axis along the n-fold axis (n is a positive integer). The components in an axis system $S2$ which is obtained by rotating $S1$ over an angle $2\pi/n$ about the z-axis will be identical to the ones in $S1$:

$$V^2_q(S2) \;=\; \sum_{q'} D^{(2)}_{q'q}\left(\alpha=\frac{2\pi}{n},\,0,\,0\right)V^2_{q'}(S1) \;=\; V^2_q(S1) \tag{64}$$

Because of the following property of the Wigner rotation matrix elements:

$$D^{(2)}_{q'q}\,(\alpha,\,0,\,0) \;=\; e^{-iq\alpha}\,\delta_{q'q} \tag{65}$$

we find

$$e^{-iq\frac{2\pi}{n}}\,V^2_q(S1) \;=\; V^2_q(S1) \qquad or \qquad e^{-iq\frac{2\pi}{n}} \;=\; 1 \tag{66}$$

and therefore

$$q \;=\; nk \qquad k \;=\; 0,\,\pm1,\,\pm2,\,\pm3,\,\ldots \tag{67}$$

This leads to the following consequences:

- A 1-fold symmetry axis ($n = 1$)

  Due to 67 with $k = 0$, ±1 and ±2 all 5 components of the electric-field gradient tensor can be obtained.

- A 2-fold symmetry axis ($n = 2$)

  Now only $k = 0$ and ±1 lead to the allowed q-values 0 and ±2. The ±1 components are missing. According to equations 13 or 15, the 2-fold rotation axis might be chosen as the z-axis of a PAS.

- A '3 or more'-fold rotation axis ($n = 3$, 4 or 6)

  Here only $k = 0$ leads to an allowed $q = 0$, the other components are missing. According to equation 15 the n-fold rotation axis can be chosen as the z-axis of a PAS in which the electric-field gradient is axially symmetric ($\eta = 0$).

We can summarize our first symmetry criterion as follows: *if an electric-field gradient can exist at a given position of which the point group contains at least a 3-fold rotation axis, it will be axially symmetric about that axis.* Note that the proof does not use any properties of the lattice symmetry (space group), only of the point group. This theorem is therefore valid also for atoms and molecules (in the latter case also 5-fold and ($n \geq 6$)-fold rotation axes are possible).

With this theorem we can finally understand the gravitational examples from section 3 from hyperfinecourse A: framework. The axis system chosen for the double ring was found in equation 57 (hyperfinecourse A: framework) to be a PAS. Indeed, the z-axis is an n-fold rotation axis with $n = \infty$, and must therefore according to our theorem be the z-axis of a PAS.

3.6 Theorem 2: a cubic environment

A second theorem is this one: *whenever the point group contains more than 2 distinct ($n \geq 3$)-fold rotation axes, the electric-field gradient at the center of the point group is zero.* A proof valid for molecules and solids goes as follows: according to the first theorem, both rotation axes specify a PAS in which the field gradient is axially symmetric. Only the V_0^2-component can be different from zero in both axis systems, and according to equations 64 and 66 the value of V_0^2 is the same in both systems[10]. As there is freedom to choose the X- and Y-axes in both systems, the relation between both non-zero components is according to 63:

$$V_0^2(S1) \;=\; D_{00}^{(2)}\,(0,\,\beta,\,0)\,V_0^2(S2) \qquad V_0^2(S1) \;=\; V_0^2(S2) \tag{68}$$

with the following explicit expression for the Wigner rotation matrix element ($P_2(x)$ is the second order Legendre polynomial):

$$D_{00}^{(2)}\,(0,\,\beta,\,0) \;=\; P_2(\cos\beta) \;=\; \frac{3\cos^2\beta - 1}{2} \tag{69}$$

Equation 68 must hold for any value of V_0^2 and any value of β. This is possible only if $V_0^2(S1) = V_0^2(S2) = 0$, which makes the electric-field gradient zero.

When we restrict ourselves to crystalline solids, only the cubic point group contains the 2 required high-symmetry axes. Five different cubic point groups exist:

[10] The same conclusion can be obtained by the cartesian form: because of the PAS, both 3×3-matrices are diagonal. They must have the same eigenvalues and $|V_{zz}|$ must be the largest. Therefore both matrices must be equal.

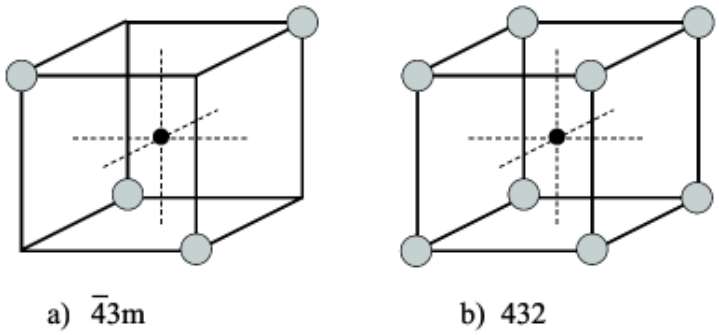

Figure 3: *a) One of the three tetrahedral point groups. b) One of the two octahedral point groups.*

- *Tetrahedral point groups:* These contain four 3-fold axes (and three 2-fold axes). There are three tetrahedral point groups: 23, $\bar{4}$3m and m$\bar{3}$ (T, T_d and T_h respectively in Schönfließnotation). An example of $\bar{4}$3m is drawn in fig. 3-a.
- *Octahedral point groups:* These contain four 3-fold axes and three 4-fold axes. There are two species: 432 and m$\bar{3}$m (O and O_h). An example of 432 is drawn in fig. 3-b.

In molecules also other point groups with the required symmetries can exist.

The inverse of the second theorem is not valid: if the field gradient appears to be zero, this does not necessarily imply the existence of two ($n \geq 3$)-fold axes. An example of this situation is the the double ring of section 3 from hyperfinecourse A: framework with $\sqrt{2}R = h$: an ∞-fold axis and lots of 2-fold axes are present, but no others. However, such situations will occur only in molecules, not in solids.

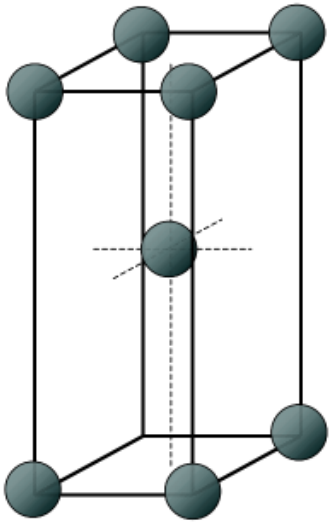

Figure 4: *Body centered tetragonal (bct) crystal structure ($a = b \neq c$).*

3.7 Examples of electric-field gradients in solids

3.7.1 The EFG in bct-In

At room temperature, pure In is a silver-grey, soft metal. It has a body-centered tetragonal lattice structure (space group I4/mmm, Fig. 4), with lattice constants a=b=3.2523 Å and c=4.9461 Å. All atoms in this structure are equivalent, and their point group is 4/mmm. This point group is lower than cubic, hence we expect an EFG at the In-site. There is a 4-fold rotation axis, hence the PAS of the EFG will have its Z-axis parallel to the 4-fold rotation axis, and there will be axial symmetry: the choice of X- and Y-axes does not matter.

3.7.2 The EFG of Fe in Fe_4N

Considering crystallographic symmetry only, one Fe-site (Fe-I) in this compound has a tetragonal point group, the other Fe-site (Fe-II) has a cubic point group. An EFG at the Fe nucleus is possible at the Fe-I site only. The point group of the Fe-I site is the same 4/mmm as in the bct-In example, hence we know immediately that the PAS of the EFG will have its Z-axis along the 4-fold rotation axis, and that there will be axial symmetry. In contrast to the case of bct-In, however, the orientation of this PAS is not the same for all Fe-I atoms (even though they are equivalent!). Indeed, for two Fe-I atoms the 4-fold rotation axis is parallel to the c-axis of the crystal, for two others it is parallel to the b-axis and for the remaining two parallel to the a-axis.

4 Miscellaneous topics

4.1 Ab initio calculations of the EFG tensor

The magnetic field at a nucleus could be separated into local contributions (Fermi, orbital and spin-dipolar contributions) and more distant contributions (Lorentz, demagnetizing and atomic-dipolar contributions). Each of the local contributions could stem from s-, p-, d- or f-electrons. For the electric-field gradient, the number of contributions is much smaller. In a mathematical description that is tailored to the so-called LAPW-method, the EFG can be divided into a contribution from electrons that 'belong'[11] to the atom that contains the nucleus under consideration, and a contribution from more distant electrons[12]. Numerical calculations show the latter contribution to be extremely small. If we want to get more physical insight in the origin of an EFG, the only thing left to do is to see how local s-, p-, d- and f-electrons contribute to this EFG of local origin. For this purpose, let us write the principal component V_{zz} of the EFG in terms of the electron charge density $\rho_e(\vec{r})$:

$$V_{zz} = <\psi_e^{(0)}|\,\hat{V}_{zz}\,|\psi_e^{(0)}> \tag{70}$$

$$= \frac{1}{4\pi\,\epsilon_0}\int \rho_e(\vec{r})\,\frac{3\cos^2\theta-1}{r^3}\,d\vec{r} \tag{71}$$

It is understood that the origin of the axis system (r=0) is at the nucleus of interest. Very close to the nucleus, where r is small, we can expect a large contribution to V_{zz} provided $\rho(\vec{r})$ is sufficiently large. However, near the nucleus the electron density is small. We could also expect the region further away from the nucleus where the highest electron density is, to be contributing most. There however $1/r^3$ is small. For a long time, it has been unclear which of both regions yield the dominant contribution. Only after sufficiently accurate *ab initio* methods became available, it could be shown that the region of small r is absolutely dominant, so dominant that contributions from charges at other atoms are irrelevant (see the discussion about the formulation in the LAPW framework given above, and the reference to P. Blaha given there). To illustrate this, first define the following function:

$$V_{zz}(r) = \frac{1}{4\pi\,\epsilon_0}\int_{|\,\vec{r}|=0}^{|\,\vec{r}|=r} \rho_e(\vec{r})\,\frac{3\cos^2\theta-1}{r^3}\,d\vec{r} \tag{72}$$

Obviously, in the limit of large r we find back the definition of V_{zz}:

$$\lim_{r\to\infty} V_{zz}(r) = V_{zz} \tag{73}$$

[11] Where one can put the boundary between this atom and neighbouring atoms is not obvious. In the LAPW-method an exact definition is used for this boundary. One should not attribute physical meaning to this boundary, however.

[12] P. Blaha, K. Schwarz, and P.H. Dederichs, *Physical Review B* **37** (1988) 2792

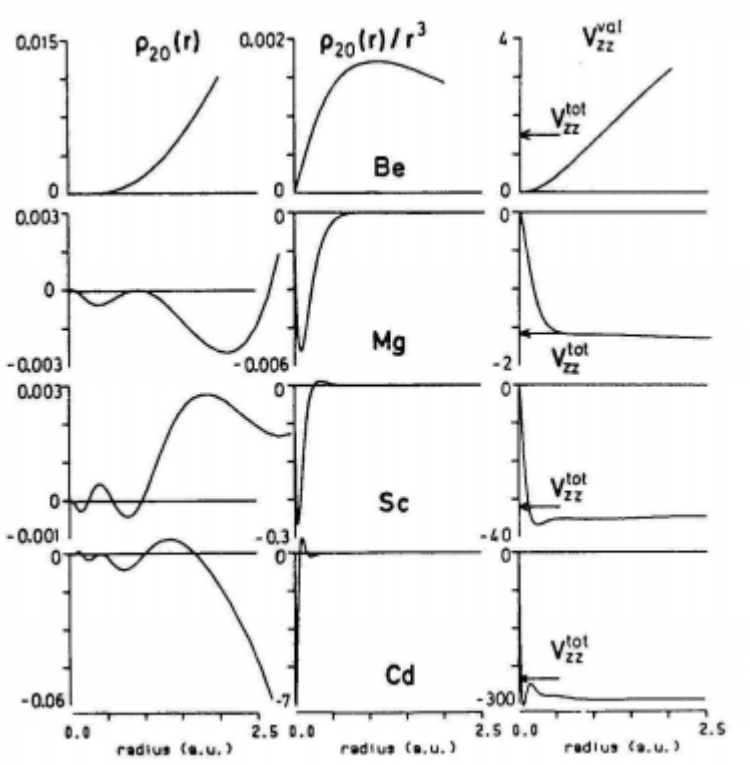

Figure 5: *Illustrating which regions in space contribute to V_{zz}. First column: the function $\rho_e(r)$ from the integrand in equation 72 (without $1/r^3$). Second column: similarly, but with the factor $1/r^3$. Third column: this function integrated up to r, which is equation 72. The arrows indicate the full calculated V_{zz}, including the "lattice contribution" from distant atoms.*

If one plots $V_{zz}(r)$ as a function of r, then in many cases the full value of V_{zz} is obtained already for $r \approx 0.2$ Å, a distance that is 10 times smaller than the radius of a typical atom. This function is plot for several pure hcp materials in Fig. 5, and except for the very light Be atom the EFG is indeed of very local nature.

Some warning words are appropriate here. We just concluded that the EFG is of very local nature. In the literature, one can find at many places statements like "the EFG is a very local property that is determined only by the first few neighbour shells of atoms". This is a statement that is not entirely true[13], and

[13]It is a statement grown under the influence of the obsolete point charge model that will be discussed in the next section.

certainly completely different from the conclusion we just arrived at. It is *true* that the EFG is a very *local* property: only the charge density in region inside the atom and very close to the nucleus determines the EFG. The properties of this part of the charge density, however, are determined by wider environment of the atom under consideration. Chemical bonds with its first nearest neighbours will have an influence on this local charge density. Chemical bonds of these neighbours with their respective neighbours will have an influence as well, through their effect on the properties of the nearest neighbours which will influence the bonds with the original atom, and so on. In this way, the local charge density near the nucleus contains information on what is chemically happening in a region of several Ångstroms around the central atom, typically 5 shells of neighbours. That is still 'local' compared to a macroscopic scale, but a different kind of locality than the 0.2 Å (=deeply within an atom) involved in the relation between charge density and V_{zz}. These two concepts are often confused.

Which are now the electrons that most contribute to V_{zz}? *Ab initio* calculations have shown[14] that the integral 71 can be separated[15] in an integral over ρ_e^p, ρ_e^d and ρ_e^f. For spd-materials, the contribution due to the valence p-electrons is often dominant, even for transition metals that do not have native valence p-electrons. For lanthanides and actinides, the f-contribution becomes dominant if the f-electrons are localized.

Interestingly, these calculations show how a very old, intuitive model to understand the EFG – the Townes-Dailey approximation[16] – has a sound, physical basis. In the Townes-Dailey model, one makes a so-called 'asymmetry count' of the orbitals of a state, taking care of the symmetry of that state. For instance, the p-orbitals consist of 3 mutually perpendicular lobes (p_x, p_y and p_z, see Fig. 6). In a crystal with axial symmetry along the z-axis, the occupation of p_x and p_y will be identical, and different from the occupation of p_z. If the occupation of p_z – call this n_z – is smaller than the occupation of p_x or p_y) – call this $n_x = n_y$ – then the overall p charge density will be oblate (Fig. 6). Intuitively, this corresponds to a negative V_{zz}. The 'asymmetry count' for p-states is defined as

$$\Delta_p \quad = \quad \frac{n_x}{2} + \frac{n_y}{2} - n_z \tag{74}$$

and is also negative. *Ab initio* calculations have shown that there is a fairly good proportionality between this asymmetry count (where the n_i come from calculations) and an accurately calculated p-contribution to V_{zz}. If there is charge accumulation along the Z-axis (prolate charge density), then n_z is larger

[14] See the earlier reference to P. Blaha (1988), and also S. Cottenier, V. Bellini, M. Çakmak, F. Manghi and M. Rots, *Physical Review B* **70** (2004) 155418, and references therein.

[15] Here we simplify a bit. In a correct mathematical treatment, the density can be split according to so-called Gaunt numbers, of which the densities with the p-p, d-d and f-f Gaunt numbers have the dominant contributions. These p-p density can be related to the density due to p-electrons, and therefore we note it here immediately as ρ_e^p.

[16] C.H. Townes and B.P. Dailey, *Journal of Chemical Physics* **17** (1949) 782

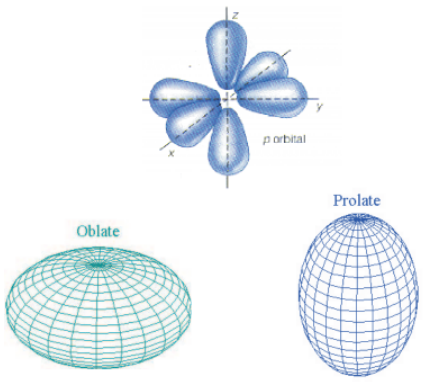

Figure 6: *Schematic picture of p-orbitals. When the occupation in the xy-plane is dominant, the overall p-charge distribution is oblate. If p-charge accumulates along the z-axis, the overall p-distribution is prolate.*

than $n_x = n_y$, and Δ_p is positive. This is in agreement with the positive V_{zz} that is expected. For a cubic environment, $n_x = n_y = n_z$, such that $\Delta_p = 0$, which is consistent with $V_{zz} = 0$ (by symmetry).

For d-electrons as well an asymmetry exists, and it is defined as:

$$\Delta_d \quad = \quad n_{xy} + n_{x^2-y^2} - \frac{1}{2}n_{xz} - \frac{1}{2}n_{yz} - n_{z^2} \tag{75}$$

For many years, *ab initio* calculations that could sufficiently accurately solve for V_{zz} were not available. How to extract physical meaning from the measured EFG's then? An attempt to classify experimental data was the *point charge model*. The underlying assumptions of this model are:

- The key feature of the EFG is the contribution from localized charges at (neighbouring) atomic sites ('lattice EFG'). [*We know meanwhile that such a contribution is negligible.*] If an assumption for the value of these localized charges (point charges) are made, the EFG due to them can be obtained by a simple summation (see further).
- This lattice EFG gets amplified by the electron orbital of the atom under consideration, who get deformed under the influence of the lattice EFG. For every element, the effect of this deformation can be expressed by a single scaling parameter (Sternheimer factor). [*We know meanwhile that the hope for the existence of such a single parameter is unjustified: Nature is much more complicated*]

Although the point charge model is incorrect and obsolete, it has been used a lot in the past and you should know how what it is about in order to understand the older literature. Below, the point charge model is explained in more detail. A critical analysis of one the failures of this model – together with the better *ab initio* interpretation – is given in S. Jalali Asadabadi, S. Cottenier, H. Akbarzadeh, R. Saki and M. Rots, *Physical Review B* **66** (2002) 195010.

Consider the nucleus of an ion, the latter having initially a spherically symmetric electron cloud (as a free ion). Put this ion at a site with lower-than-cubic symmetry in a solid. Due to this low symmetry, the positions of the neighbouring ions are such that they must generate an EFG at the nucleus of interest. Because these neighbours are outside the electron cloud of the ion, we call the principal component of this field gradient V_{zz}^{ext}. The electron cloud of the considered atom makes bonds with the neighbours. It gets therefore deformed, looses its spherical symmetry and takes the same symmetry as the neighbourhood has. This causes an extra field gradient at the nucleus *with the same PAS as the external contribution*. We can hence write the total field gradient as the external contribution times a factor:

$$V_{zz} \;=\; (1-\gamma_\infty)\, V_{zz}^{ext} \tag{76}$$

If γ_∞ is zero, the own electron cloud is not deformed. In many cases γ_∞ is considerably larger then 1 and negative, which means a strong net amplification of V_{zz}^{ext}. For this reason, γ_∞ is called the Sternheimer *antishielding* factor. It is a property which depends only on the considered atom of ion, and reflects the latter's reaction to an external field gradient. A table with calculated values (Hartree-Fock calculations) for a lot of ions can be found in F.D. Feiock and W.R. Johnson, *Physical Review* **187** (1969) pp. 39. Some examples for important atoms are: Fe: -5.244, Sn: -22.34, Cd: -29.27.

Often situations occur where a nonspherical charge distribution is present *within* the electron cloud of the considered atom. In an ionic solid, insulator or semiconductor, this can happen for instance due to a not completely filled 4f-shell. In metals it can be due to conduction electrons penetrating into the atomic volume. In both cases this will yield an *internal* (to the atom) or *local* field gradient with principal component V_{zz}^{loc}. It will again take over the symmetry of the existing $(1-\gamma_\infty)\, V_{zz}^{ext}$ and have therefore the same PAS. The other electrons inside the atomic volume will be deformed by this internal charge distribution, and change the original V_{zz}^{loc}. Now the change is described by a parameter R, which appears to be rather small ($-0.2 \leq R \leq +0.2$), and the total principal component becomes:

$$V_{zz} \;=\; (1-\gamma_\infty)\, V_{zz}^{ext} + (1-R)\, V_{zz}^{loc} \tag{77}$$

It is quite straightforward to get a meaningful number for V_{zz}^{ext}. The neighboring nuclei screened by their electron cloud will appear from a certain distance as point charge Δe, where Δ is the extra number of electrons being at the ion. In ionic solids, Δ is an integer (positive or negative), in metals it is a fractional number. From the result for the gravitational example, we obtain the electric-field gradient tensor for a single point charge Δe at a position $\vec{r}$ from the nucleus ($-Gm_2 \rightarrow \Delta e/4\pi\epsilon_0$, $\rho_2(\vec{r}_2) \rightarrow \delta(\vec{r}_2 - \vec{r})$) in cartesian coordinates[17]. Summing over all ions in the crystal gives:

$$V^{ext} = \frac{e}{4\pi\,\epsilon_0} \sum_i \frac{\Delta_i}{r_i^3} \begin{bmatrix} \frac{3x_i^2}{r_i^2} - 1 & \frac{3x_i y_i}{r_i^2} & \frac{3x_i z_i}{r_i^2} \\ \frac{3x_i y_i}{r_i^2} & \frac{3y_i^2}{r_i^2} - 1 & \frac{3y_i z_i}{r_i^2} \\ \frac{3x_i z_i}{r_i^2} & \frac{3y_i z_i}{r_i^2} & \frac{3z_i^2}{r_i^2} - 1 \end{bmatrix} \tag{78}$$

It is of course not possible to extend the summation really to all ions in the crystal. Usually one calculates first all the matrices due to the first nearest neigbors, then of the second neighbor shell, and so on. As r_i becomes larger, the contributions become smaller and smaller, and the sum will converge. Convergence is very slow however, because shells far away will usually contain many atoms. Short-cuts exist to obtain with less effort (= faster convergence) the same final matrix[18], and for some types of lattices even analytical expressions exist[19].

Anyway, after having found the matrix for V^{ext} – in this context called also often V^{latt}, *latt* from lattice – one can find its PAS by doing a matrix diagonalization. After suitably renaming the axes, one obtains finally a value for V_{zz}^{ext}. If one is interested only in the PAS and not in the magnitude of V_{zz}, then it is sufficient to carry out the summation in 78 only over as many neighbors as is needed to obtain the symmetry of the point group, and do the diagonalization of this matrix.

Because γ_∞ is known from tabulations, we have now a procedure to obtain the external (or lattice) contribution to the electric-field gradient. Such a transparent method does not exist for the local contribution however. Based upon the then available experimental data, Raghavan *et al.*[20] concluded in 1975 that

[17] Point charges cannot occur at the same position of the nucleus, the correction term with $\rho_e(\vec{0})$ is therefore zero.

[18] F. W. De Wette, *The Physical Review* 123 (1961) p. 103, F. W. De Wette and G. E. Schacher, *The Physical Review* 137 (1965) p. A78 and p. A92, and D. B. Dickmann and G. E. Schacher, *Journal of Computational Physics* 2 (1967) p. 87.

[19] For instance, for the Cu-position in a $AuCu_3$-type of structure, one can prove that

$$V^{ext} = V^{latt} = \frac{e\,8.67}{4\pi\epsilon_0\,a_0^3}\,(\Delta_{Au} - \Delta_{Cu}) \tag{79}$$

with a_0 being the lattice constant. (G.P. Schwartz and D.A. Shirley, *Hyperfine Interactions* **3** (1977) 67)

[20] R. S. Raghavan, E. N. Kaufmann and P. Raghavan, *Physical Review Letters* 34(20) (1975) p. 1280

the local contribution in metals (here the local contribution is due to conduction electrons) is proportional to the antishielded lattice contribution and has the other sign, the universal proportionality constant $-K$ being about -3:

$$(1-R)V_{zz}^{loc} \;=\; V_{zz} - (1-\gamma_\infty)\,V_{zz}^{latt} \;=\; -K\,(1-\gamma_\infty)\,V_{zz}^{latt} \tag{80}$$

and hence

$$V_{zz} \;=\; (1-K)\,(1-\gamma_\infty)\,V_{zz}^{latt} \tag{81}$$

This 'universal correlation' with the data set of Raghavan *et al.* is shown in fig. 7-a. In later experiments[21] many exceptions to this plot have been found (for instance by Enrst *et al.*[22], fig. 7-b), making the proportional behaviour far less universal as was once thought. Fig. 7-c shows the available data set in 1983 (R. Vianden).

[21] See R. Vianden, *Hyperfine Interactions* **15/16** (1983) 189-201 for a discussion, and R. Vianden, *Hyperfine Interactions* **35** (1987) 1079-1118 for a tabulation of many more electric-field gradient measurements.

[22] H. Ernst, E. Hagn, and E. Zech, *Physical Review B* **19** (1979) 4460-4469

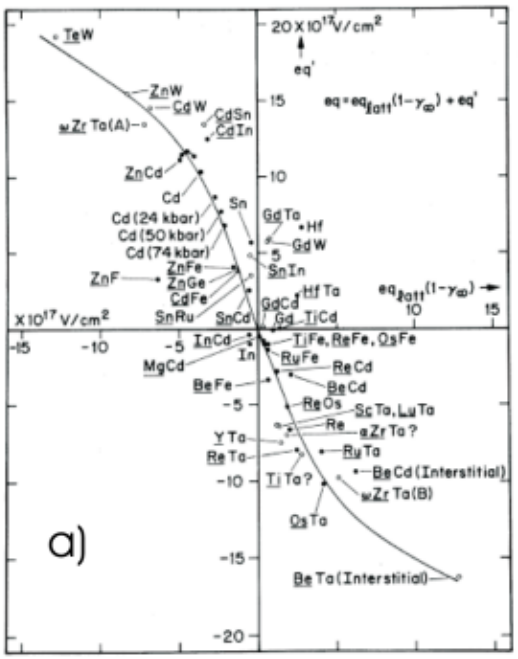

FIG. 1. Correlation of ionic and extraionic field-gradients in metals. Most values refer to room temperature. A typical temperature dependence is shown in the case of *Zn*Cd by an arc of data points. Underlined symbols refer to the host metal. *A* and *B* refer to two inequivalent substitutional sites in ω-Zr. Filled circles indicate data from e^2qQ values of known signs. For open circles, e^2qQ signs are unknown. Locations of these points are predicted.

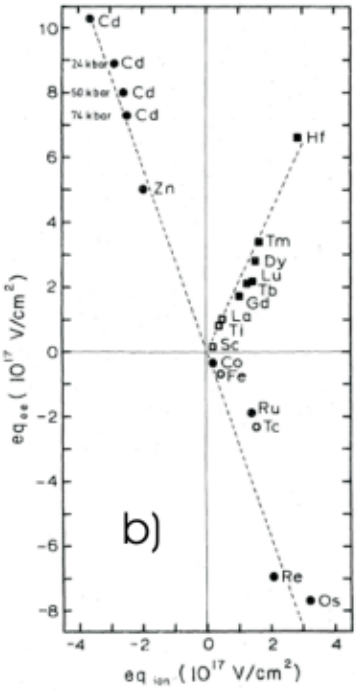

FIG. 7. Correlation of ionic and electronic contributions to the total electric field gradient in pure hexagonal metals. Circles indicate data from group-II*b*, -VIII*b*, and -VIII*b* metals, squares indicate data from group III*b* and IV*b* metals. Open symbols refer to data with unknown signs, their locations are predicted.

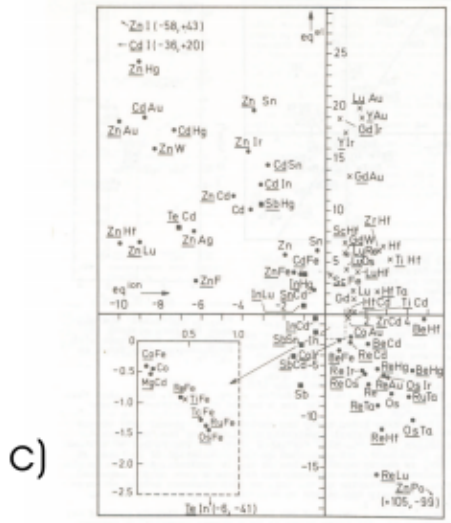

Fig. 4 Plot of eq^{el} versus eq^{ion} for all systems known today. Open 4f shell rare earth and some systems far outside the range of the figure (Tm2, ReTe, Re3) have been omitted. Different symbols are used for different atomic groups of host metals: ● group II, IIIb, VIIb and VIIIb, ✖ group IIIb and IVb, ■ group III, V and VI.

Figure 7: *Pictures of pretended correlations between the total electric-field gradient and the point-charge lattice contribution (with their original captions), with data sets available in 1979 [a): Raghavan, b): Ernst] and 1983 [c): Vianden]. See text for detailed references.*

4.2 Temperature dependence of the electric-field gradient

Up to now we did not mention temperature. In almost all cases, the electric-field gradient lowers when the temperature raises. Fig. 8 shows V_{zz} as a function of temperature for Cd(Cd), Sn(Cd), and Ru(Cd). The kind of temperature dependence is not the same in all classes of materials however. Regular spd-compounds follow a $T^{1.5}$-law:

$$V_{zz}(T) = V_{zz}(0)\left(1 - BT^{1.5}\right) \tag{82}$$

There is no formal justification for the exponent 1.5 and actual values may differ from 1.5 slightly. The factor B has the order of magnitude of $10^{-4} - 10^{-5}K^{-1.5}$. It is highly surprising that so many cases – equation 82 holds equally well for pure compounds as for the field gradient on impurities – can be described by such a simple formula, which contains only a single free parameter ($V_{zz}(0)$ is trivial).

In materials with f-electrons, the temperature dependence is linear:

$$V_{zz}(T) = V_{zz}(0)\left(1 - BT^{1}\right) \tag{83}$$

Broad studies do not exist, but it seems this linear behaviour remains even if the electric-field gradient is measured at a position where no f-atom sits, as the field gradient on ^{111}Cd on the Sn-position in USn_3.

The final picture to understand these temperature dependences at a fundamental level has not yet been worked out. Of course, the field gradient must become smaller if the lattice expands. This effect is too small however to explain the observed temperature variation. Next, one could think about an electronic effect. The higher the temperature is, the more electrons are thermally excited. The bonds which were sharply defined at 0K become hence more and more blurred. 'Blurred' means that spherical symmetry of the electron cloud is more and more restored, and the electric-field gradient will therefore become smaller. But the temperatures needed for this to be an observable effect are orders of magnitude higher than the temperature range of fig. 6-7***. The only remaining possibility is the influence of lattice vibrations (phonons), which indeed are important in the range of 0 - 1000 K. The fact that for impurities in a host-lattice the observed B correlates with the Debye-temperature of the host is an experimental support for this. The final theory to describe $V_{zz}(T)$ will therefore have to deal with phonons in an accurate way (An early and rather successful model for the electron-phonon coupling can be found in P. Jena, *Physical Review Letters* **36** (1976) 418-421 and in D. R. Torgeson and F. Borsa, *Physical Review Letters* **37** (1976) 956-959. Other references can be found in E. N. Kaufmann and R. J. Vianden, *Review of Modern Physics* 51(1) (1979) p. 161, in W. Witthuhn and W. Engel in *Hyperfine Interactions of Radioactive Nuclei*, ed. J. Christiansen, pp. 205-280, 1983, Springer-Verlag, ISBN 3-540-12110-2, in R. Vianden, *Hyperfine Interactions* **15/16** (1983) 189-201, and H. C. Verma and G. N. Rao, *Hyperfine Interactions* **15/16** (1983) 207-210.).

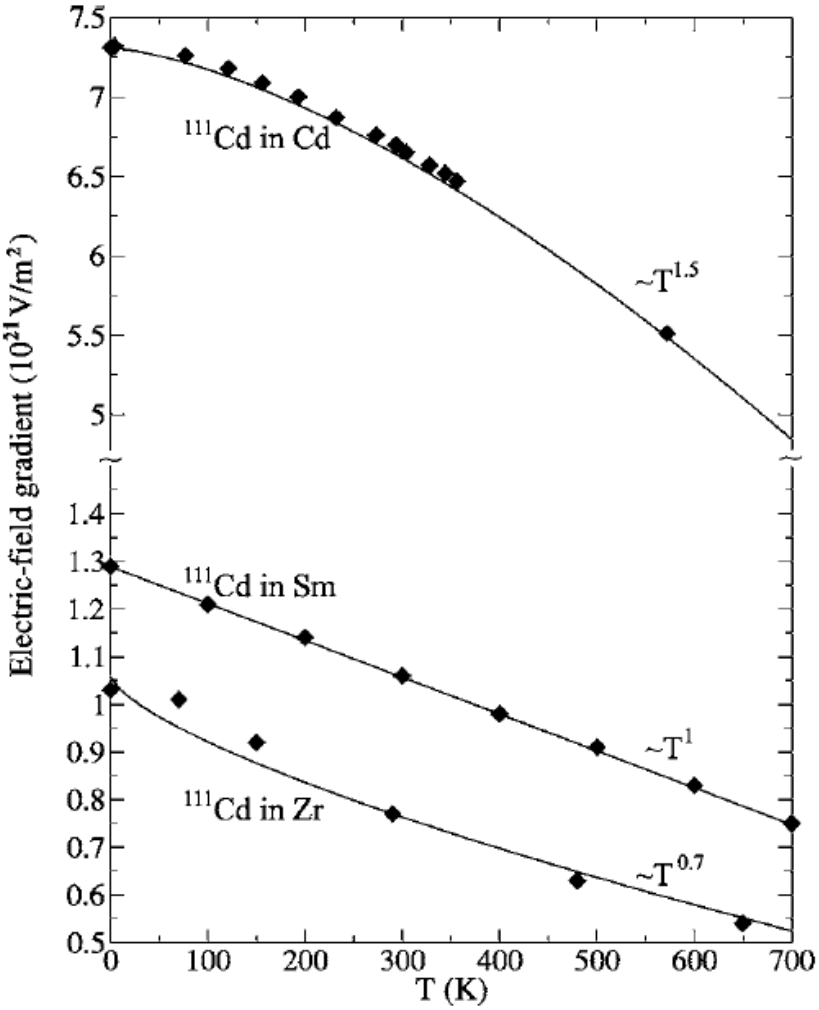

Figure 8: *T-dependence of $V_{zz}(T)$=$V_{zz}(0)$(1-BT^{α}) (solid lines are fits through the experimental values) for Cd(Cd), Sm(Cd), and Zr(Cd). Phys. Rev. B (2006) 144304*

5 Combined interaction

We are ready now to combine the results of this document and the previous one and study the interaction between a nucleus and a magnetic field and electric-field gradient that are present simultaneously. We will discuss the case of solids only. The general solution of this problem is complex, and we will restrict ourselves to a few manageable cases. Cases which are not treated are explicitly mentioned, in order to indicate clearly what is missing here. An important note to make is that a lot of steps use formulas not previously discussed[23]. As the online course only goes briefly over this subject (and not in a strong mathematical way whatsoever), it is more important to understand the different cases than to follow the mathematics behind them.

5.1 General formulation

Consider a nucleus with angular momentum $I \geq 1$, observable magnetic dipole moment μ (or alternatively, g-factor g), and observable electric quadrupole moment Q. Both μ (or g) and Q can be either positive or negative. This nucleus is inside a solid, and feels a magnetic field $\vec{B}(\vec{0})$ and an electric-field gradient $\vec{V}(\vec{0})$ that are fixed with respect to the crystal lattice. The crystal is described in an axis system that is fixed with respect to e.g. the experimental apparatus that is used to study the nucleus, and is therefore sometimes called the LAB-system. Our static $\vec{B}(\vec{0})$ can be described in this LAB-system by 3 components B_x, B_y and B_z. There will be a PAS in which $\vec{B}(\vec{0})$ has only one non-zero component. In order to specify $\vec{V}(\vec{0})$ with respect to the LAB-system, 5 components are needed. Equation 11 shows that also here a PAS can be chosen such that only 3 non-zero components remain (with only 2 degrees of freedom). The description of $\vec{B}(\vec{0})$ and $\vec{V}(\vec{0})$ is simplest in their PAS, but these two PAS in general do not coincide. We will have to choose one of them, and accept the complications for the other interaction which we cannot describe in its PAS.

As we assume $\vec{B}(\vec{0})$ and $\vec{V}(\vec{0})$ to be known quantities, we can again formulate a nuclear Hamiltonian. Diagonalization of the matrix of its matrix elements will lead to the eigenvalues and eigenstates. The general nuclear magnetic Hamiltonian in an axis system not necessarily being the PAS associated with $\vec{B}(\vec{0})$:

$$\hat{H}_{jj}^{nuc} = -\frac{g_I \mu_N}{\hbar} \vec{B}(\vec{0}) \cdot \hat{\vec{I}} \tag{84}$$

The corresponding quadrupole hamiltonian we calculated up to now only in the PAS of the field gradient, in equation 41. By equations 3, 37 and 25 to 27 we can obtain the spherical form in a general axis system:

$$\hat{H}_{qq}^{nuc} = \frac{eQ}{2I(2I-1)\hbar^2} \left[\left(3\hat{I}_z^2 - \hat{I}^2 \right) < V_0^2 >$$

[23] We are not talking about derivations but about e.g. certain transformation formulas.

$$\mp \sqrt{\frac{3}{2}} \left(\hat{I}_z \hat{I}_{\pm 1} + \hat{I}_{\pm 1} \hat{I}_z \right) < V^2_{\pm 1} > \; + \sqrt{\frac{3}{2}} \hat{I}^2_{\pm} < V^2_{\pm 2} > \Bigg] \tag{85}$$

with $\left\langle V_q^2 \right\rangle = \left\langle \Psi_e^{(0)} \right| \hat{V}_q^2 \left| \Psi_e^{(0)} \right\rangle$.

The general problem is now to find the nuclear eigen states and eigen values of $\hat{H}^{nuc}_{jq} = \hat{H}^{nuc}_{jj} + \hat{H}^{nuc}_{qq}$. We will solve this problem in a few special cases.

6 Dominant quadrupole interaction

We first focus on the case where the quadrupole interaction is dominant. 'Dominant' means that if both interactions would act alone, ΔE^{nuc}_{qq} is much larger than ΔE^{nuc}_{jj} (equivalently: $\omega_0 \gg \omega_L$). It is a natural choice then to take the PAS of the electric-field gradient as reference system. If exact calculations would appear to be impossible, the magnetic interaction can be considered to be a perturbation to the quadrupole interaction.

6.1 The collinear case

6.1.1 Axial symmetry

This is the most simple case, and can be solved exactly: $\vec{B}(\vec{0})$ is parallel to the z-axis of the PAS of the electric-field gradient, the latter being axially symmetric. This z-axes of both PAS coincide, and for none of them the choice of x- and y-axes matters, such that both PAS can be chosen to be identical. Under these circumstances, 84 reduces to eq. 31 from hyperfinecourse A: magnetic hyperfine interaction, and 85 to 41 with $\eta = 0$:

$$\hat{H}^{nuc}_{jq} = \frac{e\,Q\,V_{zz}}{4\,I(2I-1)\,\hbar^2} \left(3\hat{I}_z^2 - \hat{I}^2\right) \; - \; \frac{g_I \mu_N}{\hbar} B(\vec{0})\, \hat{I}_z \tag{86}$$

This hamiltonian is already diagonal in the $|\, I,\, m_I >$-basis, with eigenvalues:

$$\begin{aligned} E^{nuc}_{jq}(m_I) &= \frac{e\,Q\,V_{zz}}{4\,I(2I-1)} \left(3m_I^2 - I(I+1)\right) \; - \; g_I \mu_N B\, m_I & (87) \\ &= \hbar\omega_Q \left(3m_I^2 - I(I+1)\right) \; + \; \hbar\omega_L m_I & (88) \end{aligned}$$

The energy level scheme for $I = 5/2$ is given in fig. 7-1*** for $QV_{zz} > 0$ and $g_I B < 0$. This scheme inverts whenever QV_{zz} or $g_I B$ changes sign. The $\pm m_I$ degeneracy from the quadrupole-only case is lifted.

Equation 87 is an exact solution, and does not depend on E_M being small with respect to E_Q. It even holds equally well for the case with dominating magnetic interaction.

Let us examine what happens if one increases B. For particular field strengths,

some energy levels will coincide. From 87 you can derive that $E_{QM}(m_I) = E_{QM}(m'_I)$ if:

$$\frac{\omega_L}{\omega_Q} = -3\,(m_I + m'_I) \tag{89}$$

Apparently, for a given ω_Q several ω_L exist for which this condition holds (fig. 7-2***). For instance, for the situation given in fig. 7-1***, the first coincidence will obviously happen for the levels $m_I = -3/2$ and $m_I = +1/2$. This will be if $\omega_L/\omega_Q = 3$. Such crossings of two levels are crucial for the *Level Mixing Resonance* method, a method which is especially useful to measure hyperfine interaction energies when combined interactions are present.

6.1.2 No axial symmetry

If $\vec{B}(\vec{0})$ and $\vec{V}(\vec{0})$ are collinear, but without axial symmetry for $\vec{V}(\vec{0})$, we are in a situation much similar to section 3.3 from hyperfinecourse A: magnetic hyperfine interaction. We will have the complexity of the non-zero non-diagonal elements, which are exactly the same however as in said section. Only the diagonal elements are changed, due to an additional term from the magnetic interaction. Finding the eigen values will proceed along the same scheme as presented in said section. For half-integer I, if B is sufficiently small a Zeeman-splitting of the degenerate $\pm m_I$ levels will show up. For integer I, almost degenerate levels will Zeeman-split too, and non-degenerate levels will change their mutual distance a little (increase or decrease).

6.2 The non-collinear case

6.2.1 Axial symmetry

Now consider an axially symmetric quadrupole interaction, being much stronger than a magnetic interaction and *not collinear* with it. The PAS of the magnetic hyperfine field can be specified with respect to the PAS of the electric-field gradient by the Euler angles (α, β, γ). α is an orientation about the direction of axial symmetry of the electric-field gradient. Due to this axial symmetry, α should not matter and we can choose the X- and Y-axis of the electric-field gradient PAS such that $\alpha = 0$. Similarly, γ is a rotation about the direction of the magnetic hyperfine field, which is always a direction of axial symmetry because the hyperfine field is a vector. We can choose the X'- and Y'-axis of the magnetic PAS such that $\gamma = 0$. Hence, a simplified set of Euler angles that specifies the magnetic PAS with respect to the electric PAS is (0, β, 0).

We will work in the electric PAS, and therefore we should express the magnetic hyperfine field in the electric PAS. The latter plays the role of the 'new' axis system in the transformation, such that in order to transform, we should know the Euler angles that specify the electric PAS with respect to the magnetic PAS. These are (0, $-\beta$, 0). In the 'old' (magnetic) axis system, the cartesian components of the magnetic hyperfine field are (0, 0, B). The corresponding

spherical tensor that describes the hyperfine field in the magnetic PAS has only one non-zero component: $B_0^1 = B$. Three components in the electric PAS are:

$$B_q^1(\beta) = \mathcal{D}_{0q}^1(0, -\beta, 0)\, B_0^1 \tag{90}$$

$$= (-1)^q \sqrt{\frac{4\pi}{3}}\, B\, Y_q^1(-\beta,\, 0) \tag{91}$$

Explicit expressions are:

$$B_0^1(\beta) = B\cos\beta \tag{92}$$

$$B_{\pm 1}^1 = \mp\frac{B}{\sqrt{2}}\,\sin\beta \tag{93}$$

The spherical form of the nuclear angular momentum operator $\hat{\vec{I}} = \left(\hat{I}_x,\, \hat{I}_y,\, \hat{I}_z\right)$, is :

$$\hat{I}_0^1 = \hat{I}_z \tag{94}$$

$$\hat{I}_{\pm 1}^1 = \mp\frac{1}{\sqrt{2}}\,\hat{I}_\pm \tag{95}$$

Working out the dot product in equation 84 but using spherical components, we find the desired expression:

$$H_{jj}^{nuc}(\beta) = -\frac{g_I \mu_N B}{\hbar}\left(\frac{1}{2}\sin\beta\left(\hat{I}_+ + \hat{I}_-\right) + \cos\beta\,\hat{I}_z\right) \tag{96}$$

The combined hamiltonian H_{jq}^{nuc} is not diagonal any more in the $|\, I,\, m_I >$ basis. The non-zero matrix elements depend on β and are:

$$\langle I,\, m_I|\, H_{jq}^{nuc}(\beta)\,|I,\, m_I\rangle = \hbar\omega_Q\left(3m_I^2 - I(I+1)\right) + \hbar\omega_L m_I\cos\beta \tag{97}$$

$$\langle I,\, m_I|\, H_{jq}^{nuc}(\beta)\,|I,\, m_I \pm 1\rangle = \frac{\hbar\omega_L}{2}\sin\beta\,\sqrt{I(I+1) - m_I(m_I \pm 1)} \tag{98}$$

Due to the off-diagonal matrix elements, the $|\, I,\, m_I >$-states are no eigen states any more. In our first order perturbation procedure where H_{jq}^{nuc} is the perturbing Hamiltonian (with V_{zz} and B the small parameters) with respect to the dominant monopole Hamiltonian, the following matrix must be diagonalized in order to find the new eigen states ($I = \frac{5}{2}$ as an example):

$$\begin{array}{c} +\frac{5}{2}\;\; +\frac{3}{2}\;\; +\frac{1}{2}\;\; -\frac{1}{2}\;\; -\frac{3}{2}\;\; -\frac{5}{2} \\ \left[\begin{array}{cccccc} qj & j & 0 & 0 & 0 & 0 \\ j & qj & j & 0 & 0 & 0 \\ 0 & j & qj & j & 0 & 0 \\ 0 & 0 & j & qj & j & 0 \\ 0 & 0 & 0 & j & qj & j \\ 0 & 0 & 0 & 0 & j & qj \end{array}\right] \end{array} \tag{99}$$

The symbol 'qj' indicates a contribution due to H_{qq}^{nuc} and H_{jj}^{nuc} simultaneously, the symbol 'j' a contribution due to H_{jj}^{nuc} only.

If the quadrupole interaction is dominant, we can apply first order perturbation theory a second time. We can take the monopole Hamiltonian plus H_{qq}^{nuc} as the unperturbed Hamiltonian, and H_{jj}^{nuc} as the perturbation with B as the small parameter ($B \ll V_{zz}$). Under the unperturbed Hamiltonian, the $\pm m_I$ states are degerate:

$$\begin{bmatrix} \langle m_I | H_{jj}^{nuc} | m_I \rangle & \langle m_I | H_{jj}^{nuc} | -m_I \rangle \\ \langle -m_I | H_{jj}^{nuc} | m_I \rangle & \langle -m_I | H_{jj}^{nuc} | -m_I \rangle \end{bmatrix} \tag{100}$$

For $m_I = \frac{5}{2}$ and $m_I = \frac{3}{2}$, this is a diagonal matrix: the eigenstates are unchanged, and the degenerate eigenvalues split (their separation is $2\hbar\omega_L m_I \cos\beta$). For $m_I = \frac{1}{2}$, the matrix is not diagonal:

$$\frac{\hbar\omega_L}{2} \begin{bmatrix} \cos\beta & k \sin\beta \\ k \sin\beta & -\cos\beta \end{bmatrix} \tag{101}$$

with $k = \sqrt{I(I+1) + \frac{1}{4}}$. It is left as an exercise to diagonalize this and find the separation between the two levels.

Note finally that when $\vec{B}(\vec{0})$ is perpendicular to the Z-axis of the PAS of the quadrupole interaction and small, the energies in first order are unaffected, except for $m_I = \pm\frac{1}{2}$.

6.2.2 No axial symmetry

We do not deal with the case of a dominant non-axially symmetric quadrupole interaction combined with a non-collinear magnetic interaction. Note only that now matrix elements with $\Delta m_I = \pm 1$ and $\Delta m_I = \pm 2$ are present in the $|\, I, m_I >$-basis.

7 Dominant magnetic interaction

7.1 The collinear case

7.1.1 Axial symmetry

We already dealt with this case, as the axially symmetric quadrupole interaction with collinear magnetic interaction was solved exactly, irrespective of the relative strength of both interactions.

7.1.2 No axial symmetry

This will not be discussed.

7.2 The non-collinear case

7.2.1 Axial symmetry

If the Z-axis of the PAS of a small electric quadrupole interaction is not parallel to the Z-axis of the PAS of a large magnetic interaction, we better take the latter PAS as our reference frame, and express the quadrupole interaction in this axis system. The magnetic hamiltonian of equation 84 simplifies to:

$$\hat{H}_{jj}^{nuc} = -\frac{g_I \mu_N}{\hbar} B \hat{I}_z \tag{102}$$

while the quadrupole hamiltonian is given in 85. The magnetic PAS is our final reference system here, and the orientation of the electric PAS with respect to the magnetic PAS is specified by the Euler angles (α, β, γ). For the same reasons as in section 6.2.1, the axes can be taken such that α and γ are zero, without loosing generality[24]. We will not make this choice, however. We will start out with general values for all three Euler angles, in order to demonstrate that – with somewhat more work – the α- and γ-dependence will disappear spontaneously from the equations.

First we transform the single non-zero component of the electric-field gradient tensor from its PAS to the magnetic PAS. In order to do so, we need the Euler angles that specify the magnetic PAS with respect to the electric PAS: $(-\gamma, -\beta, -\alpha)$. The transformed components are:

$$\begin{aligned} \left\langle V_q^2 \right\rangle_M &= D_{0q}^{(2)}(-\gamma, -\beta, -\alpha) \left\langle V_0^2 \right\rangle_E & (103) \\ &= d_{0q}^2(-\beta)\, e^{iq\alpha} \left\langle V_0^2 \right\rangle_E & (104) \\ &= \frac{(-1)^q}{2} \sqrt{\frac{4\pi}{5}}\, e^{iq\alpha}\, Y_q^2(-\beta, 0)\, V_{zz} & (105) \end{aligned}$$

(the subscripts M and E indicate components in the magnetic and electric PAS, respectively). The γ-dependence has already disappeared. Now, fill this out in

[24] Note that α and γ are not the same angles as in section 6.2.1: α is now a rotation about the magnetic hyperfine field.

equation 85 in order to find the quadrupole hamiltonian in the magnetic PAS as a function of V_{zz}, α, and β:

$$H_{qq}^{nuc} = \frac{eQ\,V_{zz}}{4I(2I-1)\hbar^2}\left[\underbrace{\frac{3\cos^2\beta-1}{2}\left(3\hat{I}_z^2-\hat{I}^2\right)}_{\hat{a}\,'}\right.$$
$$\left.\underbrace{+\sqrt{\frac{3}{2}}\sin\beta\,\cos\beta\left(\hat{I}_z\hat{I}_{\pm1}+\hat{I}_{\pm1}\hat{I}_z\right)}_{\hat{b}_\pm}\;e^{\pm i\,\alpha}\;+\;\underbrace{\sqrt{\frac{3}{8}}\sin^2\beta\,\hat{I}_\pm^2}_{\hat{c}_\pm}\;e^{\pm 2i\,\alpha}\right] \quad (106)$$

The matrix elements of the total hamiltonian $H_{jj}^{nuc}+H_{qq}^{nuc}$ in the $|\,I,\,m_I>$-basis, now depend on β and α (to simplify notation, assume we are dealing with $I=2$):

$$H(\alpha,\,\beta) = \frac{eQ\,V_{zz}}{4I(2I-1)\hbar^2}\begin{bmatrix} a & b_+\,e^{i\alpha} & c_+\,e^{2i\alpha} & 0 & 0 \\ b_-\,e^{-i\alpha} & a & b_+\,e^{i\alpha} & c_+\,e^{2i\alpha} & 0 \\ c_-\,e^{-2i\alpha} & b_-\,e^{-i\alpha} & a & b_+\,e^{i\alpha} & c_+\,e^{2i\alpha} \\ 0 & c_-\,e^{-2i\alpha} & b_-\,e^{-i\alpha} & a & b_+\,e^{i\alpha} \\ 0 & 0 & c_-\,e^{-2i\alpha} & b_-\,e^{-i\alpha} & a \end{bmatrix} \quad (107)$$

with a the appropriate matrix element of $\hat{a}$, etc. The symbol a is chosen such that the magnetic interaction is correctly incorporated:

$$\hat{a} = \hat{a}\,' - \frac{g_I\,\mu_N\,B\,4I(2I-1)\,\hbar}{eQV_{zz}}\,\hat{I}_z \quad (108)$$

This matrix contains both the magnetic and electric interaction in the diagonal, only the electric interaction in the two side diagonals, and zeros elsewhere. Furthermore, the symbols a, $b_\pm$ and $c_\pm$ depend on β, but not on α. Diagonalization yields the eigenvalues and eigenvectors. This diagonalization can be achieved by a suitable unitary transformation[25]:

$$H^d(\beta,\,\alpha) = U(\beta,\,\alpha)\,H(\beta,\,\alpha)\,U^{-1}(\beta,\,\alpha) \quad (110)$$

where H^d is diagonal in the new basis, and U is a unitary matrix. Next we prove that $U(\beta,\,\alpha)$ can be factorized into a β- and a α-dependent matrix: $U(\beta,\,\alpha) = U\,'(\beta)\,A(\alpha)$. Indeed, one can apply the following unitary transformation which leaves a matrix $H\,'(\beta)$ depending not on α any more:

$$H\,'(\beta) = A(\alpha)\,H(\beta,\,\alpha)\,A^{-1}(\alpha) \quad (111)$$

[25] A unitary transformation of the square matrix B is defined as the operation needed to obtain another square matrix A by

$$A = U\,B\,U^{-1} \quad (109)$$

with U being a unitary matrix, i.e. $U^\dagger = U^{-1}$. ($U^\dagger$ is the conjugate transpose of U).

$$\begin{bmatrix} a & b_+ & c_+ & 0 & 0 \\ b_- & a & b_+ & c_+ & 0 \\ c_- & b_- & a & b_+ & c_+ \\ 0 & c_- & b_- & a & b_+ \\ 0 & 0 & c_- & b_- & a \end{bmatrix} = A(\alpha) \begin{bmatrix} a & b_+\, e^{i\alpha} & c_+\, e^{2i\alpha} & 0 & 0 \\ b_-\, e^{-i\alpha} & a & b_+\, e^{i\alpha} & c_+\, e^{2i\alpha} & 0 \\ c_-\, e^{-2i\alpha} & b_-\, e^{-i\alpha} & a & b_+\, e^{i\alpha} & c_+\, e^{2i\alpha} \\ 0 & c_-\, e^{-2i\alpha} & b_-\, e^{-i\alpha} & a & b_+\, e^{i\alpha} \\ 0 & 0 & c_-\, e^{-2i\alpha} & b_-\, e^{-i\alpha} & a \end{bmatrix} A^{-1}(\alpha)$$

$$A(\alpha) = \begin{bmatrix} e^{2i\alpha} & 0 & 0 & 0 & 0 \\ 0 & e^{i\alpha} & 0 & 0 & 0 \\ 0 & 0 & 1 & 0 & 0 \\ 0 & 0 & 0 & e^{-i\alpha} & 0 \\ 0 & 0 & 0 & 0 & e^{-2i\alpha} \end{bmatrix} \tag{112}$$

In general, $A(\alpha)$ is constructed such that its diagonal runs from $e^{Ii\alpha}$ till $e^{-Ii\alpha}$. As $H'(\beta)$ does not depend on α, the unitary matrix $U'(\beta)$ needed to transform it into H^d will also be β-dependent only. And as an immediate consequence, $H^d(\beta)$ and its eigenvalues will not depend on α too. The complete unitary transformation looks like:

$$H^d(\beta) = \underbrace{U'(\beta)A(\alpha)}_{U(\beta,\,\alpha)}\, H(\beta,\,\alpha)\, \underbrace{A^{-1}(\alpha)U'^{-1}(\beta)}_{U^{-1}(\beta,\,\alpha)} \tag{113}$$

In this way we formally proved that for an axially symmetric electric-field gradient, the eigenvalues of the combined interaction do not depend on α, a property which we said in the beginning was intuitively obvious.

Up to now, we did not require the electric interaction to be small. If we do so, we can use first order perturbation theory, and examine how the magnetic energy levels will change under the influence of the electric interaction. The eigenstates of the unperturbed (=magnetic) hamiltonian are the $|\, I,\, m_I >$-states, the energy corrections E_c are:

$$E_c = < I,\, m_I |\, H_Q |\, I,\, m_I > \tag{114}$$

$$= \hbar\omega_Q\, \frac{3\,\cos^2\beta - 1}{2}\, \left(3m_I^2 - I(I+1)\right) \tag{115}$$

If $\beta = 0°$, we retrieve the exact expression for the collinear case we found previously. The distance between $\pm m_I$-levels remains always constant, unregardless the perturbation. There is also a so-called 'magic angle' $\beta_m \approx 54.74°$ for which $3\cos^2\beta_m - 1 = 0$: for this angle, the original magnetic levels are not changed in first order.

7.2.2 No axial symmetry

And this one we skip again.

8 None of both interactions dominant

Let us finally sketch how to treat the most general case, where none of both interactions is dominant, where the orientation of the Z-axes of both principle axis systems is arbitrary and where the electric-field gradient may have no axial symmetry. Most of the procedure we can copy from previous reasoning.

It does not matter which of both axis systems we take, assume we work in the PAS of the magnetic interaction and specify the electric PAS with respect to this magnetic PAS by Euler angles (α, β, γ). We can transform the electric-field gradient from its PAS to the magnetic PAS (for which you have to use the Euler angles ($-\gamma$, $-\beta$, $-\alpha$)). Contrary to equation 103, the electric-field gradient has V_0^2 and $V_{\pm 2}^2$ as non-zero components in its PAS (below indexed by P). The 5 components in the general axis system (below indexed by G) will therefore *all* depend on both V_{zz} and η:

$$< V_q^2 >_G = D_{0q}^2 < V_0^2 >_P + D_{2q}^2 < V_2^2 >_P + D_{-2q}^2 < V_{-2}^2 >_P \quad (116)$$

$$= d_{0q}^2(-\beta) e^{iq\alpha} < V_0^2 >_P + e^{i2\gamma} d_{2q}^2(-\beta) e^{iq\alpha} < V_2^2 >_P + e^{-i2\gamma} d_{-2q}^2(-\beta) e^{iq\alpha} < V_{-2}^2 >_P \quad (117)$$

Note that the angle γ (rotation about the electric-field gradient principal axis) does not disappear now. The 5 explicit expressions are (V_{zz} and η are with respect to the PAS of the electric-field gradient):

$$< V_0^2 >_G = \frac{1}{4}\sqrt{\frac{5}{\pi}} V_{zz} \left(\frac{3\cos^2\beta - 1}{2} + \frac{\eta}{2} \cos 2\gamma \, \sin^2\beta \right) \quad (118)$$

$$< V_{\pm 1}^2 >_G = \frac{1}{8}\sqrt{\frac{5}{3\pi}} V_{zz} \sin\beta \, e^{\pm i\alpha} \left(\pm 3\cos\beta + \sqrt{\frac{1}{2}}\,\eta \, \left[e^{-i2\gamma}(1 \mp \cos\beta) - e^{+i2\gamma}(1 \pm \cos\beta) \right] \right) \quad (119)$$

$$< V_{\pm 2}^2 >_G = \frac{1}{16} V_{zz} \sqrt{\frac{30}{\pi}} \, e^{\pm i2\alpha} \left(\sin^2\beta + \frac{\eta}{6} \left[e^{i2\gamma}(1 \pm \cos\beta)^2 + e^{-i2\gamma}(1 \mp \cos\beta)^2 \right] \right) \quad (120)$$

The matrix formed by the matrix elements will have the same structure as we encountered in the case with dominant magnetic interaction and axial symmetry, and in exactly the same way the α-dependence can be removed. The eigenvalues will hence depend on γ and β, contrary to the case with axial symmetry. No perturbation theory can be applied now, and therefore the full diagonalization by searching the suitable unitary transformation has to be performed. With some writing effort, you can write down explicitly the matrix elements for instance for $I = 3/2$. You will see that they are complex if $\eta \neq 0$.

It can be proven also that some mutual orientations of magnetic and electric interactions yield the same eigenvalues.

9 Examples

9.1 Fe_4N

The ferromagnetic compound Fe_4N was discussed already in sections hyperfinecourse A: magnetic hyperfine interaction 5.1 and 3.7.2, where we have seen that at the Fe-I sites both a hyperfine field and an electric-field gradient are present. Experimental values are about 25 T for the hyperfine field, and $2.9{\cdot}10^{21}$ V/m^2 for V_{zz}. If we would measure[26] this interaction with the first excited nuclear level of the ^{57}Fe isotope (I=3/2, g_I=-0.1553 μ_N, Q=0.16 b), then the ratio $\omega_0/\omega_L = 0.09$: we are in the situation with dominant magnetic interaction. If the magnetic moments are along the (001) direction, then the angle between the Z-axes of the magnetic and electric PAS is 0° for 2 out of 6 Fe-I atoms (Fe-Ia), while it is 90° for the other 4 (Fe-Ib). Fe-Ia can be treated with the exact equations from section 7.1, while for Fe-Ib the perturbation approach from section 7.2 can be used (it would be a good illustration to compare the energies of the 4 m-levels in both cases).

With the moments along the (111) direction, the angle between both Z-axes is the magic angle of 54.74° for all 6 Fe-I atoms, and we should use the formulae from section 7.2. Verify that the levels are identical to the Zeeman splitting from a pure magnetic interaction.

10 Epilogue

Congratulations, you have reached the end of part A. I hope you had as much fun as I did making these documents. I would like to thank S. Cottenier and M. Rots for the initial syllabus on which these documents are based. S. Cottenier deserves extra thanks for correcting and steering these documents where needed. N. Steyaert gets my appreciations for his emotional support.

That will be all. Have fun in the next section where we learn the practical applications of these tiny energy differences. And good luck in your physics/engineering/... futures.

PS I didn't make the same kind of documents for part B as I am more interested in the theory (part A) than the applications. This does not mean that they aren't as important, certainly in our daily lives. I hope these documents inspire and give some other students the courage to do the same for part B.

[26] This is *almost* what happens in a Mössbauer experiment, although there also the ground state I=1/2 level plays a role.